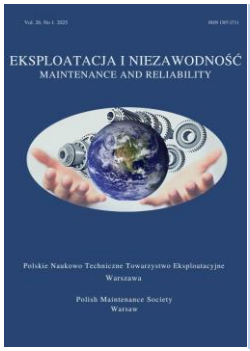

Eksploatacja i Niezawodnosc – Maintenance and Reliability

Volume 27 (2025), Issue 1

journal homepage: http://www.ein.org.pl

Article citation info:
Wei J, Liu Z, Sun Y, Wang X, An active learning method for structural reliability combining response surface model with Gaussian process of residual fitting and reliability-based sequential sampling design, Eksploatacja i Niezawodnosc – Maintenance and Reliability 2025: 27(1) http://doi.org/10.17531/ein/193443

An active learning method for structural reliability combining response surface model with Gaussian process of residual fitting and reliability-based sequential sampling design

Indexed by: Web of Science Group

Jianbao Wei[a], Zhijie Liu[a,*], Yuhang Sun[a], Xiaobang Wang[a]

[a] Dalian Maritime University, China

Highlights

- A response surface model with the adaptive residual fitting strategy is proposed to estimate the structural reliability.
- The random moving uniform design method is proposed for the surrogate model construction.
- A learning function that considers the feasibility of sample points is introduced.

Abstract

It is quite challenging to attain an accurate reliability estimation on complex structures with low computational burden. Therefore, an active learning method combining the response surface model with the Gaussian process (GP) of residual fitting and reliability-based sequential sampling design is proposed for structural reliability analysis. This method first utilizes a random quadrilateral grid to perturb the uniform design sampling and generates a small set of initial design of experiments (DoE) to establish a high-precision initial response surface model efficiently. Then, a GP model for residual prediction is constructed by using the residuals of the initial response surface model, which allows the response surface function to be closer to the limit state function (LSF). Further, a reliability-based expected improvement (REI) learning function, which inherits the property of the EI function and considers the probability of feasibility of the samples, is developed for the selection of the most feasible points to update the response surface model and the GP model. The importance sampling (IS) combined with the proposed method is employed to assess the rare failure probability of structures. Ultimately, five numerical examples are used to validate the accuracy and efficiency of the proposed method.

Keywords
structural reliability analysis, active learning, sampling strategy, surrogate model, residual fitting

1. Introduction

In practical engineering, there exist various types of random uncertainties, such as material properties, assembly errors, and random loads, which directly affect structural safety. The structural reliability analysis (SRA) aims to evaluate the safety degree of a system by considering the above uncertainties. However, the reliability analysis is limited by sample sizes and strongly nonlinear limit state function (LSF), making it difficult to efficiently solve by traditional reliability estimation methods [1,2].

The approximate analytical method is common for SRA, which mainly includes the first-order reliability method (FORM) [3] and the second-order reliability method (SORM) [4]. FORM is to replace the original function with the first-order approximate Taylor expansion expression. This method often

(*) Corresponding author.
E-mail addresses: J. Wei, wjb2022@dlmu.edu.cn, Z. Liu, liuzj@dlmu.edu.cn, Y. Sun, syh-2021@dlmu.edu.cn, X. Wang. wxb@dlmu.edu.cn

has low accuracy when dealing with high-dimensional nonlinear problems. SORM uses a second-order Taylor expansion approximation to replace the original function. However, the SORM calculation is far more complex than the FORM, and is not suitable for complex engineering problems [5]. Monte Carlo simulation (MCS) is one of the most stable and accurate simulation reliability analysis methods. However, MCS requires frequent calls to the performance function or numerical model, which leads to a low efficiency in dealing with strongly nonlinear problems [6]. Several improved MCS methods were developed to improve the efficiency, such as importance sampling (IS) [7,8], subset simulation (SS) [9], line sampling (LS) [10], and the directional sampling method (DS) [11]. These methods mainly achieve computational cost savings by limiting the sample size for evaluating the probability of failure to the required local accuracy. However, while dealing with high-dimensional or strongly nonlinear problems, these methods are still time-consuming due to high-frequency repetitive simulation calculations [12].

In recent years, the surrogate model is widely used for SRA, which can capture the complex mapping relationships between inputs and outputs, including response surface method (RSM) [13,14], radial basis function (RBF) [15,16], Kriging [17,18], support vector machine (SVM) [19,20], artificial neural network (ANN) [21,22], and Gaussian random process (GRP) [23,24]. Among them, RSM has received extensive attention from scholars in the field of reliability, due to the advantages of simple principle, high computational efficiency, and easy operation[25,26]. However, RSM tends to have insufficient ability to deal with strongly nonlinear LSFs [27]. Given the above problems, Roussouly et al. [28] proposed a sparse RSM to handle approximation error. Li et al. [29] introduced an improved quasi-sparse response surface model using the weighting method for low-dimensional simulation. Romer et al. [30] proposed an incremental experimental design method based on progressive lattice sampling (PLS) to progressively upgrade the RSM and estimate the approximate error contained in the response surface. Rathi et al. [31] proposed a response surface construction method based on the moving least squares method, which assigns higher weights to the most probable failure point (MPFP) to make the response surface function closer to the LSF at MPFP. Although the above works have made significant contributions to the application of RSM in SRA, the poor accuracy still needs to be improved for strongly nonlinear problems.

Based on the above research, it is found that RSM cannot fully capture the characteristics of nonlinear problems due to the characteristics of its construction principle, resulting in large residual values. Furthermore, the residual values in RSM increase with the increase of the non-linearity of LSFs and present an uncertain trend. Inspired by this, residual values can be seen as a set of random variables distributed in the spatial domain [32,33], which can be represented by Gaussian random processes to provide accurate predictions for RSM. So this paper develops a response surface model with GP of residual fitting to solve the structural reliability problems with implicit LSFs. In addition, for most SRA methods, accurately establishing the LSF only requires a precise determination whether the function value is positive or negative [34]. This has led to the active learning methods based on surrogate models gradually becoming the mainstream method for complex SRA problems [35,36].

In summary, this paper introduces a novel active learning method that combines the response surface model with the Gaussian process of residual fitting and reliability-based sequential sampling design. Specifically, the algorithm follows the general process of active learning methods, which mainly includes initial experimental design, surrogate model construction, reliability assessment, learning function criteria, and stopping criteria. To improve the accuracy and efficiency of the initial surrogate model, this paper proposes a random moving uniform design method (RMUDM) by combining random moving quadrilateral grid samplings with uniform samplings. The training points obtained by the RMUDM will be of uniformity and randomness, which provides high-quality sample points for the construction of the surrogate model. To achieve global sequence updates of the model and consider the reliability of new sample points, this paper proposes a reliability-based expected improvement (REI) learning function criterion that takes reliability into account in the iterative process while selecting new points and allows infilling samples to explore the solutions with a high level of reliability. Finally, case studies are conducted to compare the proposed method with several typical reliability analysis methods.

The remaining sections are organized as follows. Section 2 introduces the principles of RSM, GP model, and IS method as well as the proposed RMUDM and REI. Section 3 describes the main steps of the proposed method. In Section 4, several examples are given to validate the superiority of the proposed method. Section 5 gives the conclusions.

2. Methodology

In this section, the theoretical methods employed in the proposed method are introduced, including improved sampling methods, surrogate model methods, learning function strategies, and reliability assessment methods.

2.1. RMUDM

The fitting ability and accuracy of RSM are largely affected by the distribution of the training points in the space. Due to the lack of randomness and inability to estimate the main and interactive effects, the uniform design method (UDM) cannot effectively describe practical problems. Therefore, this paper proposes an improved UDM that uses a random quadrilateral grid to perturb the uniform design sampling. Assuming that the initial sample set has n-dimensional design variables with the boundaries being $l_i \le x_i \le u_i, i = 1,2,\cdots,n$ and the number of levels in the i_{th} dimension as q_i. The RMUDM can be described as follows:

Step 1. The original design space is randomly reduced according to the dimensions and levels of variables, it can be denoted as [37]

$$\hat{u}_i = u_i - \alpha \frac{l_i - u_i}{q_i - 1}, i = 1,2,\cdots,n \quad (1)$$

$$\hat{l}_i = u_i + \alpha \frac{l_i - u_i}{q_i - 1}, i = 1,2,\cdots,n \quad (2)$$

where α is the random reduction coefficient, $\alpha = \frac{1}{2+rand}, rand \in [0,1]$, and u_i and l_i denote the upper and lower limits of variable values in the *i*-th dimension.

Step 2. The samples are generated by the uniform method in the random reduced space via an uniform design table.

Step 3. To ensure the randomness of the samples, the resulting uniform samples are added to a random movement, which can be denoted as

$$d_i = \frac{\gamma_{ij}}{\lambda} \frac{l_i - u_i}{q_i - 1} \quad (3)$$

where $\gamma_{ij} = rand(q_i, 1)$ is the coefficient of motion, and λ is the coefficient of random movement, $\lambda = 2 + rand, rand \in [0,1]$. To ensure the uniform distribution of sample points, the minimum distance between any two adjacent random moving sample points should satisfy Eq. (4), i.e.

$$d \ge \min_{1 \le i \le m} \left[\frac{l_i - u_i}{2(q_i - 1)} \left(1 - \frac{1}{q_i - 1} \right) \right] \quad (4)$$

Step 4. If the sampling point jumps out of reduced bounds, the value of the sample is equal to the near-boundary value.

2.2. The polynomial RSM

RSM is one of the most effective and representative surrogate models, and it can substitute actual structural LSFs with a simple polynomial function. It is assumed that the initial DoE is k n-dimensional samples $x = [\boldsymbol{x}_1, \boldsymbol{x}_2, \cdots, \boldsymbol{x}_k]^{\mathrm{T}}$, and corresponding response values are $\boldsymbol{Y} = [G(\boldsymbol{x}_1), G(\boldsymbol{x}_2), \cdots, G(\boldsymbol{x}_k)]^{\mathrm{T}}$. The first-order model expression of RSM is

$$\hat{G}(\boldsymbol{x}) = a_0 + \sum_{i=1}^{n} \boldsymbol{b}_i \boldsymbol{x}_i + \boldsymbol{\varepsilon} \quad (5)$$

where $\boldsymbol{x}_i$ is the basic variable, n is the number of variables, a_0 and $\boldsymbol{b}_i$ are undetermined coefficients solved by the least-squares fit, and $\boldsymbol{\varepsilon}$ is the random error.

The most widely used mathematical expression of response surfaces with interactive terms is

$$\hat{G}(\boldsymbol{x}) = a_0 + \sum_{i=1}^{n} \boldsymbol{b}_i \boldsymbol{x}_i + \sum_{i=1}^{n} \boldsymbol{c}_i \boldsymbol{x}_i^2 + \sum_{\substack{i,j=1 \\ j>i}}^{n} \boldsymbol{d}_{ij} \boldsymbol{x}_i \boldsymbol{x}_j + \boldsymbol{\varepsilon} \quad (6)$$

where $\boldsymbol{x}_i$ is the basic variable, n is the number of variables, a_0, $\boldsymbol{b}_i$, $\boldsymbol{c}_i$, and $\boldsymbol{d}_{ij}$ are the undetermined coefficients solved by the least-squares fit.

In general, to reduce the computing efforts, the quadratic interactive terms are not considered, Eq. (6) can be simplified to Eq. (7):

$$\hat{G}(\boldsymbol{x}) = a_0 + \sum_{i=1}^{n} \boldsymbol{b}_i \boldsymbol{x}_i + \sum_{i=1}^{n} \boldsymbol{c}_i \boldsymbol{x}_i^2 + \boldsymbol{\varepsilon} \quad (7)$$

According to the definition of RSM, an unified polynomial model can be described as

$$\hat{G}(\boldsymbol{x}) = \sum_{i=1}^{k} \boldsymbol{\omega}_i \boldsymbol{x}_i + \boldsymbol{\varepsilon} \quad (8)$$

where $\boldsymbol{\omega}_i$ is the undetermined coefficient, and k is the minimum number of test points required to determine the undetermined coefficient. It is determined based on the form of the response surface, for example, the three typical cases as shown in Table 1 where n is the number of design variables.

Table 1 shows the number of terms in the polynomial response surface model, which increases with the number of

variables, especially for quadratic functions with interactive terms. To obtain the coefficient $\boldsymbol{\omega}_i$, k independent experiments need to be conducted. The estimated value of the response surface at that test point is obtained by incorporating m test points$x^{(i)}, i = 1,2,\cdots,m$ into Eq. (9):

$$\hat{G}(\boldsymbol{x}) = \sum_{i=1}^{k} \boldsymbol{\omega}_i \boldsymbol{x}_i^{(j)}, j = 1,2,\cdots,m \quad (9)$$

Usually, to save computational resources, the interactive terms are discarded during the construction of the polynomial response surfaces model, but this behavior greatly reduces the accuracy of RSM in practical applications. To demonstrate the robustness of the proposed method in dealing with problems with and without interactive terms, specific examples will be analyzed and explained in Section 4.

Table 1. Form of response surface functions and the number k of undetermined coefficients $\boldsymbol{\omega}_i$.

Form	Number (k)
linear function	$k = n + 1$
Separable quadratic function (Excluding interactive terms)	$k = 2n + 1$
Complete quadratic function (Including interactive terms)	$k = \frac{(n+1)(n+2)}{2}$

2.3. GP model

The GP surrogate model accurately approximates functions in high-dimensional space and has been used in the field of SRA. Similarly, as for k n-dimensional samples and corresponding response values $Y = [G(x_1), G(x_2), \cdots, G(x_k)]^T$, the GP surrogate model can be constructed for predicting unknown response points. The GP is a set of random variables. Assuming that the function to be fitted conforms to a joint multivariate Gaussian prior distribution, the GP model function can be denoted as

$$\hat{G}_{\mathrm{gp}}(\boldsymbol{x}) = \mu_{\mathrm{gp}} + z_{\mathrm{gp}}(\boldsymbol{x}) \quad (10)$$

where μ_{gp} is the mean of the GP surrogate model, $z_{\mathrm{gp}}(\boldsymbol{x})$ is the GP, and $E\left(z_{\mathrm{gp}}(\boldsymbol{x})\right) = 0$, the variance is $\mathrm{VAR}\left(z_{\mathrm{gp}}(\boldsymbol{x})\right) = \sigma_{\mathrm{gp}}^2$.

The covariance of $z_{\mathrm{gp}}(\boldsymbol{x})$ is denoted as

$$cov(z_{\mathrm{gp}}(\boldsymbol{x}_i), z_{\mathrm{gp}}(\boldsymbol{x}_j)) = \sigma_{\mathrm{gp}}^2 \boldsymbol{R}_{ij}^{\mathrm{gp}} (i, j = 1,2,\cdots k) \quad (11)$$

Usually, $\hat{G}_{\mathrm{gp}}(\boldsymbol{x})$ follows the multivariate normal distribution $N_{\mathrm{ns}}\left(1_{\mathrm{ns}}\mu_{\mathrm{gp}}, \Sigma\right)$ where $\Sigma = \sigma_{\mathrm{gp}}^2 R^{\mathrm{gp}}$ is the correlation matrix composed of $\boldsymbol{R}_{ij}^{\mathrm{gp}}$, and the commonly used correlation functions of Gaussian are as follows:

$$\boldsymbol{R}_{ij}^{\mathrm{gp}} = \prod_{l=1}^{d} exp\left(-\boldsymbol{\theta}_l^{\mathrm{gp}} \left|\boldsymbol{x}_{i,l} - \boldsymbol{x}_{j,l}\right|^2\right) \quad (12)$$

where $\boldsymbol{\theta}_k^{\mathrm{gp}} = (\boldsymbol{\theta}_1^{\mathrm{gp}}, \boldsymbol{\theta}_2^{\mathrm{gp}}, \cdots, \boldsymbol{\theta}_d^{\mathrm{gp}}) \in [0, \infty)^d$ is the hyperparameters vector of the GP surrogate model, the prediction of the value $\hat{\mu}_{\hat{G}}(\boldsymbol{x}_0)$ for the unknown point $\boldsymbol{x}_0$, and the uncertainty of the prediction $\sigma_{\hat{y}}^2(\boldsymbol{x}_0)$ at the point $\boldsymbol{x}_0$can be calculated by Eqs. (13) and (14).

$$\hat{\mu}_{\hat{G}}(\theta^{\mathrm{gp}}) = (1_{n_s}{}^T (\boldsymbol{R}^{\mathrm{gp}})^{-1} 1_{n_s})^{-1} (1_{n_s}{}^T (\boldsymbol{R}^{\mathrm{gp}})^{-1} Y) \quad (13)$$

$$\sigma_{\hat{y}}^2(\theta^{\mathrm{gp}}) = \frac{(\boldsymbol{Y} - \boldsymbol{1}_{n_s}\hat{\mu}_{\mathrm{gp}}(\boldsymbol{\theta}^{\mathrm{gp}}))^T (\boldsymbol{R}^{\mathrm{gp}})^{-1} (\boldsymbol{Y} - \boldsymbol{1}_{n_s}\hat{\mu}_{\mathrm{gp}}(\boldsymbol{\theta}^{\mathrm{gp}}))}{\boldsymbol{n_s}} \quad (14)$$

Similar to the empirical Bayesian regression method, GP regression uses the maximum edge likelihood strategy to obtain the optimal hyperparameters. The negative logarithmic likelihood function for the hyperparameter $\boldsymbol{\theta}_k{}^{gp}$ can be calculated by Eqs. (15) and (16).

$$-2\,log(\boldsymbol{L}_{\theta_{\mathrm{gp}}}^{\mathrm{gp}}) = log(|\boldsymbol{R}^{\mathrm{gp}}|) + n_s\, log[(\boldsymbol{Y} - \boldsymbol{1}_{ns}\hat{\mu}_{\mathrm{gp}}(\boldsymbol{\theta}^{\mathrm{gp}}))^T (\boldsymbol{R}^{\mathrm{gp}})^{-1} (\boldsymbol{Y} - \boldsymbol{1}_{ns}\hat{\mu}_{\mathrm{gp}}(\boldsymbol{\theta}^{\mathrm{gp}}))] \quad (15)$$

According to the maximum likelihood method, the optimal linear unbiased estimation at the prediction point x^* is

$$\hat{y}_{\mathrm{gp}}(\boldsymbol{x}^*) = \hat{\mu}_{\mathrm{gp}} + \boldsymbol{r}_{\mathrm{gp}}^T (\boldsymbol{R}^{\mathrm{gp}})^{-1} (\boldsymbol{Y} - \boldsymbol{1}_{n_s}\hat{\mu}_{\mathrm{gp}}) = \left[\frac{1 - \boldsymbol{r}_{\mathrm{gp}}^T (\boldsymbol{R}^{\mathrm{gp}})^{-1} \boldsymbol{1}_{n_s}}{\boldsymbol{1}_{n_s}{}^T (\boldsymbol{R}^{\mathrm{gp}})^{-1} \boldsymbol{1}_{n_s}} \boldsymbol{1}_{n_s}{}^T + \boldsymbol{r}_{\mathrm{gp}}^T\right] (\boldsymbol{R}^{\mathrm{gp}})^{-1} \boldsymbol{Y} \quad (16)$$

The corresponding mean square error is

$$s_{\mathrm{gp}}^2(\boldsymbol{x}^*) = E[(\hat{y}_{\mathrm{gp}}(\boldsymbol{x}^*) - \mathrm{y}(\boldsymbol{x}))^2] = \sigma_{\mathrm{gp}}^2 (\boldsymbol{1} - \boldsymbol{r}_{\mathrm{gp}}^T (\boldsymbol{R}^{\mathrm{gp}})^{-1} \boldsymbol{r}_{\mathrm{gp}} + \frac{\boldsymbol{1} - \boldsymbol{1}_{n_s}{}^T (\boldsymbol{R}^{\mathrm{gp}})^{-1} \boldsymbol{r}^2}{\boldsymbol{1}_{n_s} (\boldsymbol{R}^{\mathrm{gp}})^{-1} \boldsymbol{1}_{n_s}}) \quad (17)$$

where the correlation function is $\boldsymbol{r}_{\mathrm{gp}} = \left(\boldsymbol{r}_{\mathrm{gp}1}(\boldsymbol{x}^*), \boldsymbol{r}_{\mathrm{gp}2}(\boldsymbol{x}^*), \cdots, \boldsymbol{r}_{\mathrm{gp}n_s}(\boldsymbol{x}^*)\right)$, and the correlation function between different variables is $\boldsymbol{r}_{gpi} = \mathrm{corr}\left(z(\boldsymbol{x}^*), z(x_i)\right)$. During the construction of the GP model, parameters $\hat{\mu}_{\mathrm{gp}}$, θ^{gp} and σ_{gp}^2 are replaced with corresponding estimated values [38].

2.4. Reliability-based expected improvement criterion (REI)

The expected improvement (EI) criterion can realize the sequence update of the model in the global scope [39]. Assuming that the predicted response value of any point x in the m-dimensional design space follows a Gaussian distribution

$$\hat{G}(\boldsymbol{x}) = N\left(\mu_{\hat{G}}(\boldsymbol{x}), \sigma_{\hat{G}}(\boldsymbol{x})\right) \quad (18)$$

where $\hat{\mu}_G(\boldsymbol{x})$ is the mean and $\sigma_{\hat{G}}(\boldsymbol{x})$ is the standard deviation provided by the prediction model.

According to the EI criterion, the improvement of the surrogate model at sample point x can be expressed as

$$I(\boldsymbol{x}) = \max\left(G_{\min} - \hat{G}(\boldsymbol{x}), 0\right) \tag{19}$$

where $G_{\min} = \min(y_1, y_2, \cdots, y_m)$ is the minimum value of the true response value of the performance function corresponding to the MCS sample point and $\hat{G}(\boldsymbol{x})$ is the predicted response value at sample point $\boldsymbol{x}$.

The expectation of the sample point x on the improvement function of the surrogate model can be expressed as

$$E\left(I(\boldsymbol{x})\right) = \begin{cases} \left\{\left(G_{\min} - \hat{\mu}_G(\boldsymbol{x})\right)\Phi\left(\frac{G_{\min} - \hat{\mu}_{\hat{G}}(\boldsymbol{x})}{\sigma_{\hat{G}}(\boldsymbol{x})}\right) + \sigma_{\hat{G}}(\boldsymbol{x})\phi\left(\frac{G_{\min} - \hat{\mu}_{\hat{G}}(\boldsymbol{x})}{\sigma_{\hat{G}}(\boldsymbol{x})}\right)\right\}, \sigma_{\hat{G}}(\boldsymbol{x}) > 0 \\ 0, \qquad \sigma_{\hat{G}}(\boldsymbol{x}) = 0 \end{cases} \tag{20}$$

where $\Phi(\cdot)$ is the standard normal cumulative distribution function, and $\phi(\cdot)$is the probability density function.

With the increasing of the iterations, $G_{\min}$ gradually decreases. When $G_{\min} = 0$, it indicates that the sample is on the structural LSF, and it is regarded as the best sample. Therefore, to improve the acquisition probability of the best sample, Eq. (20) can be improved to Eq. (21) [40].

$$IE\left(I(\boldsymbol{x})\right) = \begin{cases} \left\{\left(-\hat{\mu}_G(\boldsymbol{x})\right)\Phi\left(\frac{-\hat{\mu}_{\hat{G}}(\boldsymbol{x})}{\sigma_{\hat{G}}(\boldsymbol{x})}\right) + \sigma_{\hat{G}}(\boldsymbol{x})\phi\left(\frac{-\hat{\mu}_{\hat{G}}(\boldsymbol{x})}{\sigma_{\hat{G}}(\boldsymbol{x})}\right)\right\}, \sigma_{\hat{G}}(\boldsymbol{x}) > 0 \\ 0, \qquad \sigma_{\hat{G}}(\boldsymbol{x}) = 0 \end{cases} \tag{21}$$

To further improve the efficiency of screening samples in the active learning process, the reliability-based EI function that fully considers the probability of feasibility of the desired sampling point is proposed. Given the prediction of the GP model $\hat{y}(\boldsymbol{x}) \sim N\left(\mu_{\hat{G}}(\boldsymbol{x}), \sigma_{\hat{G}}(\boldsymbol{x})\right)$, the reliability index β and the reliability of predicted points $R_{\hat{G}}(\boldsymbol{x})$ can reflect the reliability level of the predicted samples, which are defined as

$$\beta = \frac{\mu_{\hat{G}}(\boldsymbol{x})}{\sigma_{\hat{G}}(\boldsymbol{x})}, R_{\hat{G}}(\boldsymbol{x}) \approx \Phi(\beta) \tag{22}$$

The REI criterion considers both the degree of feasibility and improvement of the predicted samples. According to the sampling characteristics of the REI criterion, the location of the updated sampling point is obtained by maximizing the REI criterion, which is defined as

$$RE\left(I(\boldsymbol{x})\right) = \begin{cases} R_{\hat{G}}(\boldsymbol{x})\left\{\left(-\hat{\mu}_G(\boldsymbol{x})\right)\Phi\left(\frac{-\hat{\mu}_{\hat{G}}(\boldsymbol{x})}{\sigma_{\hat{G}}(\boldsymbol{x})}\right) + \sigma_{\hat{G}}(\boldsymbol{x})\phi\left(\frac{-\hat{\mu}_{\hat{G}}(\boldsymbol{x})}{\sigma_{\hat{G}}(\boldsymbol{x})}\right)\right\}, \sigma_{\hat{G}}(\boldsymbol{x}) > 0 \\ 0, \qquad \sigma_{\hat{G}}(\boldsymbol{x}) = 0 \end{cases} \tag{23}$$

$$x^* = \arg\max_x \left(RE\left(I(\boldsymbol{x})\right)\right) \tag{24}$$

2.5. Importance sampling (IS)

The IS method is a statistical experimental method named for its high computational efficiency and small computational efforts [41]. Its basic principle is to change the sampling center to make the sampling points having a higher likelihood of falling in the failure domain, to obtain more efficient information, and to achieve variance reduction.

In general, the failure probability $\hat{p}_f$ can be denoted as

$$\hat{p}_f = p(G(\boldsymbol{x}) \le 0) = \int_{R^n} I(\boldsymbol{x})_{F_S} f_X(\boldsymbol{x})\, d\boldsymbol{x} = \int_{G(\boldsymbol{x})\le 0} f_X(\boldsymbol{x}) d\,\boldsymbol{x} \tag{25}$$

where $\boldsymbol{x} = \{\boldsymbol{x}_1, \boldsymbol{x}_2, \cdots, \boldsymbol{x}_k\}^T$ denotes the input random variable vector, R^n represents the n-dimension variable space, $G(\boldsymbol{x})$ is the LSF, Fs is the failure region, and f_X is joint probability distribution function (PDF) of the random variables. $G(\boldsymbol{x}) \le 0$ indicates failure, and $G(\boldsymbol{x}) > 0$ indicates security. The indicator function $I(\boldsymbol{x})_{F_S}$ is defined

$$I(\boldsymbol{x})_{F_S} = \begin{cases} 1, \ \boldsymbol{x} \in \{\boldsymbol{x} | G(\boldsymbol{x}) \le 0 \\ 0, \qquad else \end{cases} \tag{26}$$

Suppose the sampling function of the IS method is $h_X(\boldsymbol{x})$, and Eq. (25) can be rewritten as

$$\hat{p}_f = \int_{R^n} I(\boldsymbol{x})_{F_S} \frac{f_X(\boldsymbol{x})}{h_X(\boldsymbol{x})} h_X(\boldsymbol{x})\, d\mathrm{x} \tag{27}$$

When the variables $\boldsymbol{x}_i$ are independent, the probability of failure $\hat{p}_f$ can be estimated using the MCS as

$$\hat{p}_f = \frac{1}{N}\sum_{i=1}^{N} I(\boldsymbol{x}^{(i)})_{F_S} \frac{f_X(\boldsymbol{x}^{(i)})}{h_X(\boldsymbol{x}^{(i)})} \tag{28}$$

where $\boldsymbol{x}_i$ is the ith sample generated from the system importance sampling function $h_x(\boldsymbol{x})$, and N is the number of samples.

3. Procedures of the proposed method

The framework of the proposed algorithm is depicted in Fig. 1 and its concrete steps are explained as follows:

Step 1. Define the initial DoE $\boldsymbol{X}_{\mathrm{DoE}} = [\boldsymbol{P}^1, \cdots, \boldsymbol{P}^N]$ with the proposed RMUDM and calculate the true LSF value $\boldsymbol{Y}_{\mathrm{DoE}}$. The size of the initial training points should be as small as possible because the additional points will be added to this DoE step by step. Noticeably, the number of initial training points is $(n+1)\cdot\frac{n+2}{2}$ at least, where n is the number of design variables.

Step 2. According to the existing DoE, establish the initial response surface prediction model $\hat{G}_1(\boldsymbol{x})$ by the least square method.

Step 3. Predict the initial $\boldsymbol{X}_{\mathrm{DOE}}$ response values $\widehat{\boldsymbol{Y}}_{\mathrm{DoE}}$ by initial response surface prediction model $\hat{G}_1(\boldsymbol{x})$. For existing DoE, calculate the residual $\boldsymbol{R}_{\mathrm{DoE}}$ between the actual values $\boldsymbol{Y}_{\mathrm{DoE}}$ by the LSF and the predicted response values $\widehat{\boldsymbol{Y}}_{\mathrm{DoE}}$ of the response surface model.

Step 4. First, transform the input variables into a standard normal distribution. Then, construct the GP prediction model $\hat{G}_{\mathrm{GP}}(\boldsymbol{x})$ by taking initial sample points $\boldsymbol{X}_{\mathrm{DOE}}$ and residual values $\boldsymbol{R}_{\mathrm{DOE}}$ as input variables and input response values, respectively.

Step 5. Obtain a new response surface model $\hat{G}_2(\boldsymbol{x})$ by adding the function of residual $\hat{G}_{\mathrm{GP}}(\boldsymbol{x})$ into the response surface model $\hat{G}_1(\boldsymbol{x})$.

Step 6. Evaluate the failure probability $\hat{p}_f$, and calculate the reliability index β. First, the prediction model $\hat{G}_2(\boldsymbol{x})$ is used to predict the sample points by IS. Then, the probability of failure is estimated with the signs of these predictions by using Eq. (28).

Step 7. Evaluate the stopping condition. If the accuracy-stopping criterion is satisfied, the algorithm goes to the last step. Otherwise, start active learning, and go to Step 8.

To ensure the adaptive convergence of the algorithm, the stopping criterion based on the reliability index β is employed to determine whether the algorithm stops or not, which can be denoted as

$$\left|\frac{\beta^n-\beta^{n-1}}{\beta^n}\right| \le \varepsilon \tag{29}$$

where β^n and β^{n-1} are the reliability index calculated for the nth and (n-1)th update, respectively, and ε is a small threshold with the value being 0.001.

Step 8. Generate the population candidate samples $\boldsymbol{S}_{\mathrm{MCS}}[x^1, x^2, \cdots, x^n]$ by MCS and identify the next best point $\boldsymbol{S}_{\mathrm{MCS}}$ to evaluate the LSF. Each sample point $\boldsymbol{S}_{\mathrm{MCS}}$ is calculated by $\hat{G}_{\mathrm{GP}}(\boldsymbol{x})$ and $\hat{G}_2(\boldsymbol{x})$, which provides prediction variances and response values to the proposed learning function REI. Then, pick the best sample points $\boldsymbol{S}_{\mathrm{MCS}}$ that satisfy $x^* = \arg\max_x \left(RE\left(I(\boldsymbol{x})\right)\right)$.

Step 9. Update the previous DoE with the best point x^*. First, remove the standardization of the new sample x^*. Then, add the new sample x^* and its actual response value by the LSF to the $\boldsymbol{X}_{\mathrm{DoE}}$. Following this, it is added to the DoE, $N_{i+1} = N_i + 1$. Then, goes back to Step 2 to update the $\hat{G}_2(\boldsymbol{x})$.

Step 10. Evaluate and output the failure probability $\hat{p}_f$.

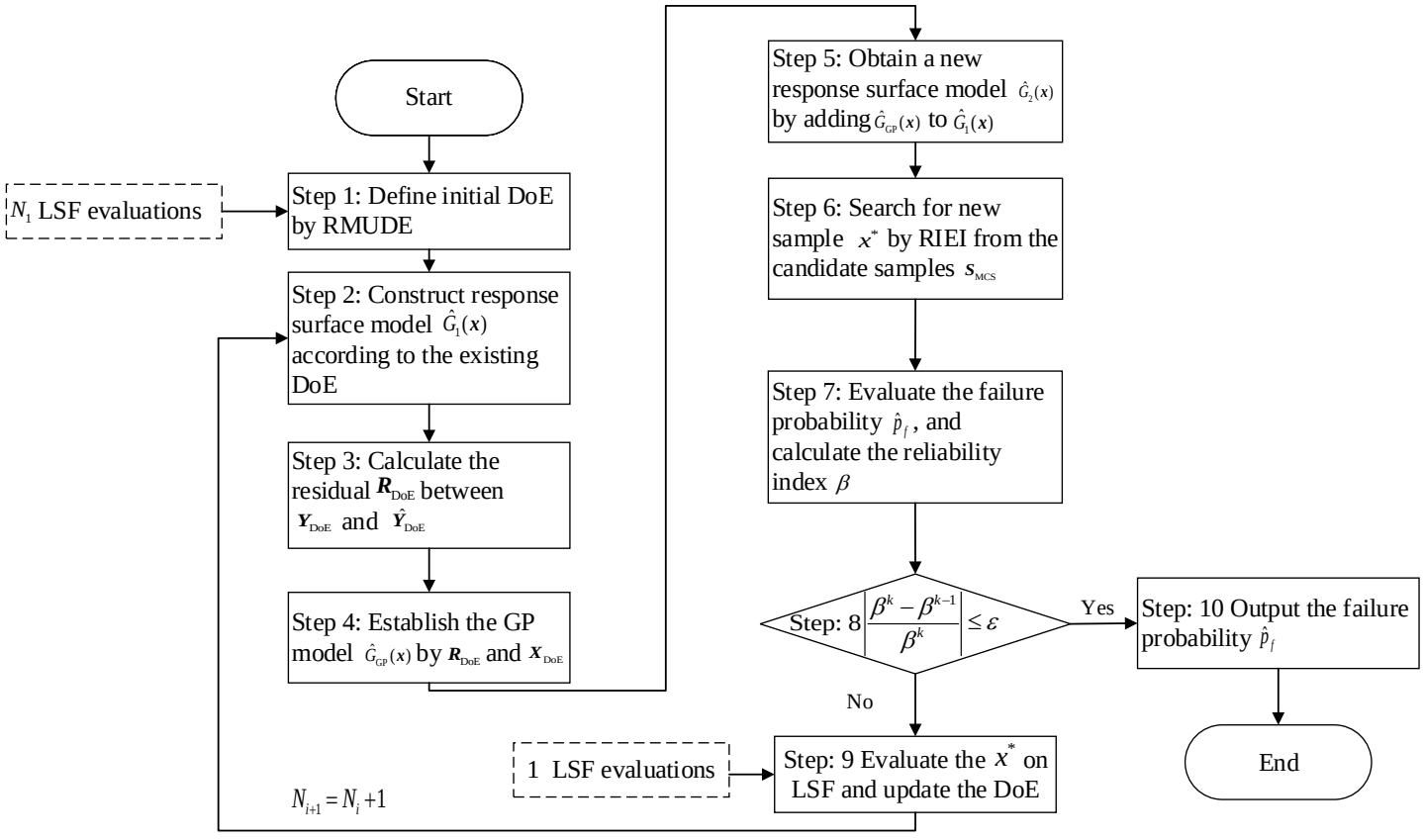

Fig. 1. The reliability analysis flowchart of the proposed method.

4. Example analysis

In this section, several examples are given to conduct a comparative study of the proposed method. The performance of the proposed method is validated by the relative error $\varepsilon_{\mathrm{MCS}}$ compared to MCS. $\varepsilon_{\mathrm{MCS}}$ can be derived by

$$\varepsilon_{\mathrm{MCS}} = \frac{|\hat{p}_f^{\mathrm{MCS}} - \hat{p}_f|}{\hat{p}_f^{\mathrm{MCS}}} \tag{30}$$

where $\hat{p}_f^{\mathrm{MCS}}$ is the failure probability obtained by MCS, and $\hat{p}_f$ is the failure probability obtained by the proposed method.

4.1. Example 1: A highly nonlinear problem

The example examines the numerical performance of the proposed approach by considering a 2D nonlinear performance function [42,43,44]:

$$g(x) = sin\frac{5x_1}{2} - \frac{(x_1^2+4)(x_2-1)}{20} + 2 \tag{31}$$

where x_1 and x_2 are two independent normal variables with unit standard deviations. The specific parameters are $x_1 \sim N(1.5,1)$ and $x_2 \sim N(2.5,1)$.

In this example, the number of initial training points is 12, and the threshold for stopping criterion is set as $[\varepsilon] = 0.001$. To reduce the uncertainty of the results, the reliability analysis method based on the proposed point addition strategy is repeated 10 times. The reference result $\hat{P}_f = 3.131 \times 10^{-2}$ for a sample size 5×10^5 is generated by the MCS method [42]. N_{call} is the number of calls to the performance function.

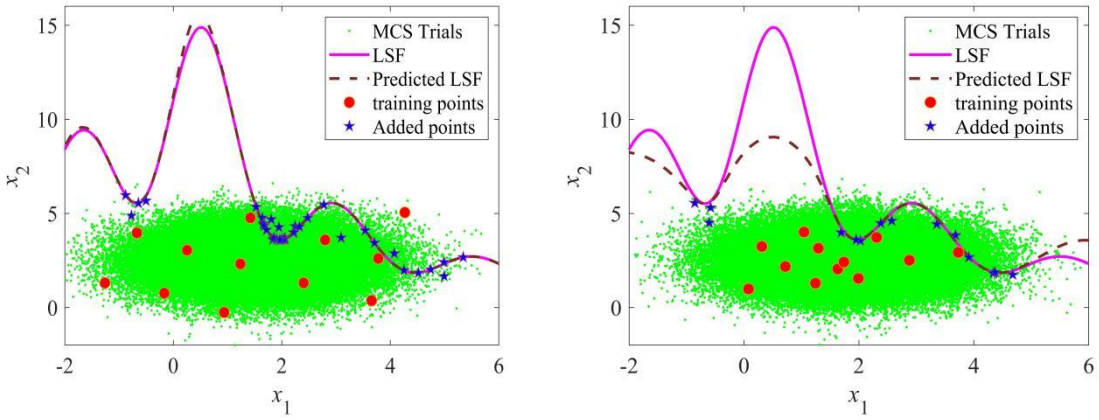

Fig. 2. Performance of the proposed method for Example 1: (a) The initial DoE obtained by RMUDM; (b) The initial DoE obtained by LHS.

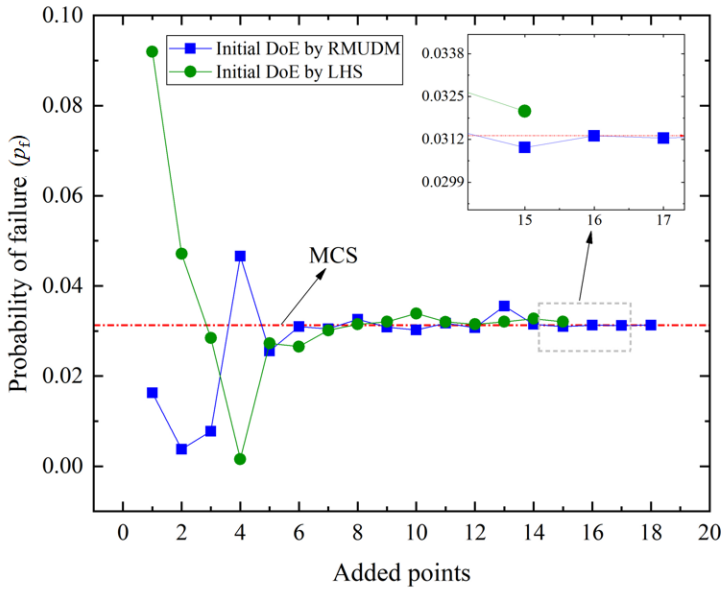

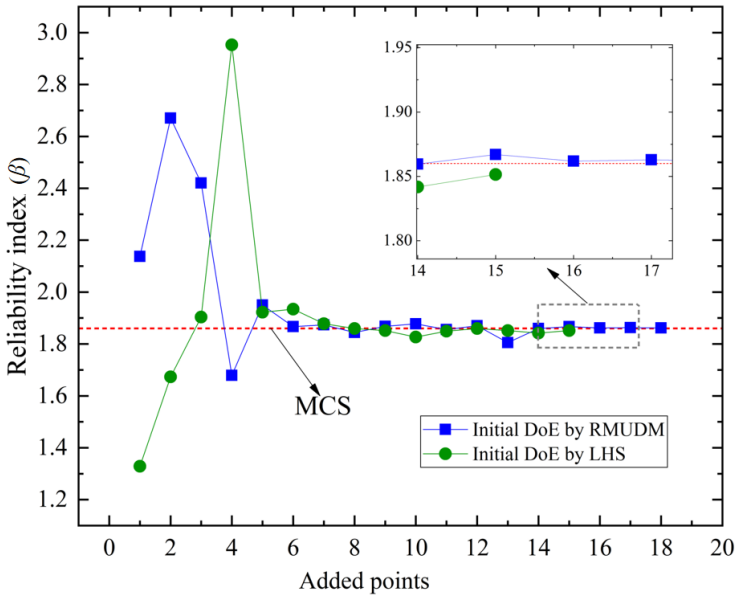

(b)

Fig. 3. Probability of failure and reliability index in the process of adding points for Example 1: (a) Probability of failure, (b) Reliability index.

The procedure of the proposed method starts with the initial DoE, and the iterative calculation of the algorithm is started by evaluation criteria. By adding new points and updating the prediction model, the prediction LSF is constructed. To prove the effectiveness of the proposed method, the initial DoE obtained by different sampling methods are used for the reliability analysis of Example 1. The results and the process are shown in Fig. 2 and Fig. 3. Fig. 2 (a) shows the predicted LSF (the black dashed line) in the region of failure probability to be evaluated is in good agreement with the original LSF (the magenta line) . Meanwhile, the added points are dispersed around the LSF, which helps to construct an effective surrogate model for reliability analysis. It is found that the initial training points obtained by the proposed RMUDM are more dispersed and have a certain randomness compared to LHS. Fig. 3 shows that the results from the initial DoE obtained by RMUDM are more consistent with the reference values in terms of failure probability and reliability index compared to LHS.

Table 2. Comparison of reliability analysis results for Example 1.

Methods	N_{call}	$\hat{p}_f$	$\varepsilon_{PF}(\%)$	β
MCS	5×10^5	3.131×10^{-2}	-	1.8619
AK-MCS+U	41	3.137×10^{-2}	0.192	1.8610
AK-MCS+EFF	37.3	3.133×10^{-2}	0.064	1.8616
Zheng et al.	38.5	3.130×10^{-2}	0.032	1.8620
Zhang et al.	37.7	3.150×10^{-2}	0.607	1.8592
Xiao et al.	76.9	3.125×10^{-2}	0.192	1.8627
Proposed method	29.5	3.135×10^{-2}	0.127	1.8613

Note: N_{call} denotes the number of calls to the limit state function, ε_{PF} denotes the percentage error of failure probability in comparison with the MCS results, and β represents the reliability index.

In this example, the proposed method is compared with six different active learning methods from Reference [42]. It is observed from Table 2, all the $\varepsilon_{PF}s$ are below 1%, which indicates that all the methods can provide accurate results. The other active learning methods listed are researched based on AK-MCS. For example, Xiao et al. [42] and Zhang et al. [44] proposed new learning functions to enhance the efficiency of reliability analysis. Optimization conditions were imposed on the U function in AK-MCS+U to obtain sample points by Zheng et al. [43]. These methods can reach a good trade-off between

accuracy and efficiency. Although the error of the proposed method is larger than that of AK-MCS+EFF and the results by Zhang et al., it has achieved accurate results with an error of less than 0.2% by utilizing the fewest calls to the LSF.

4.2. Example 2: A three-dimensional nonlinear function

This example is a three-dimensional nonlinear LSF. The basic variables x_1, x_2, and x_3 are subjected to the standard normal distributions, i.e. $x_1 \sim N(0,1)$, $x_2 \sim N(0,1)$, and $x_3 \sim N(0,1)$. The LSF is defined as

$$g(x_1, x_2, x_3) = 4 - x_1 - 0.1(x_2 + \eta\, sin(\pi x_2))^2 - 0.1(x_3 + \eta\, sin(\pi x_3))^2 \quad (32)$$

In this example, as η increases, the non-linearity of the LSF also increases. Fig. 4 shows the 3D surface of limit states with different η.

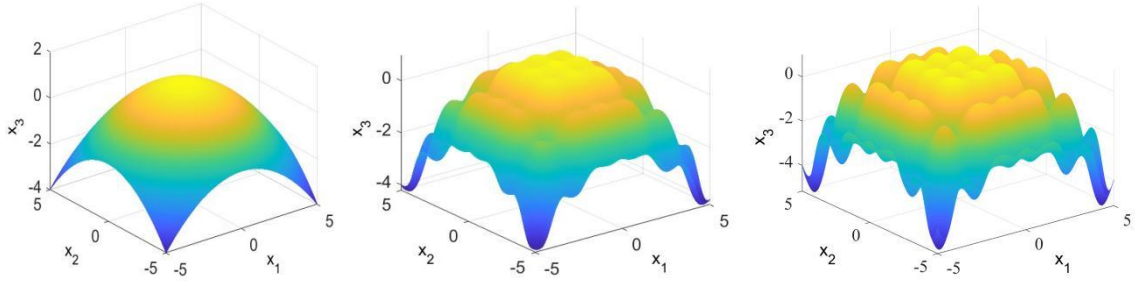

(a) (b) (c)

Fig. 4. 3D surface of limit states with different η of Example 2: (a) $\eta = 0$, (b) $\eta = 0.5$, (c) $\eta = 1$.

As the dimensions of design variables increase, the number of terms used to construct response surface models rapidly increases, especially for the interactive terms between variables. This increases the computation cost required to build the initial response surface model. If the interactive term is not considered in constructing the initial response surface model, the accuracy of the model will be affected. To demonstrate the robustness of the proposed method in SRA, the failure probability of this problem is calculated by the proposed method using initial response surface models with and without interactive terms under different parameters, and compared with the reference results by MCS. The corresponding analysis results are illustrated in Fig. 5. The sizes of both initial DoE are taken as 10 and 18, respectively.

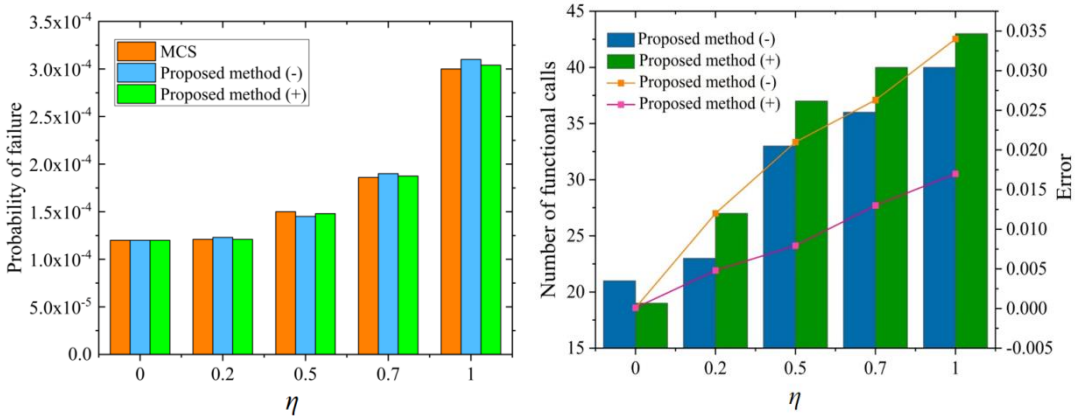

(a) (b)

Fig. 5. Reliability analysis results under different η: (a) The variation of failure probabilities, (b) The variation of the number of functional calls and the errors; Note: '+' indicates the initial response surface model with interactive terms, and '-' indicates the initial response surface model without interactive terms.

It can be seen from Fig. 5 (a) that the proposed method has strong applicability to the LSF in this example with the variation of the parameter η. However, the presence or absence of coupling terms in the initial response surface model can have an impact on the efficiency and accuracy of reliability analysis. Fig. 5 (b) shows that as η increases from 0 to 1, N_{call} and $\varepsilon_{\hat{P}_f}$ by the proposed method without interactive terms increase from 21 to 40 and 0.117% to 3.469%, respectively. And N_{call} and $\varepsilon_{\hat{P}_f}$ by

the proposed method with interactive terms increase from 19 to 43 and 0.025% to 1.614%, respectively. In addition, the proposed method without interactive terms has fewer functional calls than the proposed method with interactive terms, and its growth rate of relative error is greater. It is noted that the efficiency of the proposed method can be improved when the interactive terms are not considered in the initial response surface model, but at the cost of diminished accuracy, especially for the LSF with strong non-linearity.

Table 3. Reliability analysis results of Example 2.

Methods	N_{call}	$\hat{p}_f$	β	$\varepsilon_{PF}(\%)$
MCS	1×10^8	1.513×10^{-4}	3.6131	-
AK-MCS+U	55	1.500×10^{-4}	3.6153	0.849
AK-MCS+EFF	58	1.520×10^{-4}	3.6126	0.462
IS	2002	1.527×10^{-4}	3.6106	0.925
SS	8100	1.497×10^{-4}	3.6159	1.058
RSM	52	1.360×10^{-4}	3.6404	10.112
Proposed method (-)	33	1.480×10^{-4}	3.6188	2.181
Proposed method (+)	39	1.501×10^{-4}	3.6143	0.793

To test the applicability of the proposed method, the results of reliability for Example 2 with $\eta = 0.5$ are compared with other methods, as listed in Table 3. The reference results are calculated by MCS with a sample size of 1×10^8 and the corresponding failure probability is $\hat{p}_f = 1.513 \times 10^{-4}$. The AK-MCS+U and AK-MCS+EFF can achieve a better trade-off between accuracy and efficiency compared with IS and SS. The RSM has improved the efficiency, but the corresponding relative error is more than 10%. The proposed method with interactive terms only requires an average of 39 functional calls to reach an estimation with comparable accuracy as AK-MCS+U, AK-MCS+EFF, and IS. The proposed method without interactive terms is most efficient among the listed methods, and the maximum relative error is less than 2.2%. Overall, the proposed method is capable of achieving an outstanding trade-off between accuracy and efficiency for this strong nonlinear case. Even if the response surface model without interactive terms is used to deal with this nonlinear case, it can still get relatively reasonable results.

4.3. Example 3: Dynamic response of a nonlinear oscillator

The following example is a problem with a moderate number of random variables. It consists of a non-linear undamped single-degree-of-freedom system as shown in Fig. 6. The performance function is given as

$$g(c_1, c_2, m, r, t_1, F_1) = 3r - \left|\frac{2F_1}{m\omega_0^2} sin(\frac{\omega_0^2 t_1}{2})\right| \quad (33)$$

where $\omega_0 = \sqrt{(c_1 + c_1)/m}$ is the system frequency. Six random variables in this example follow normal distributions. The properties of all the random variables are summarized in Table 4.

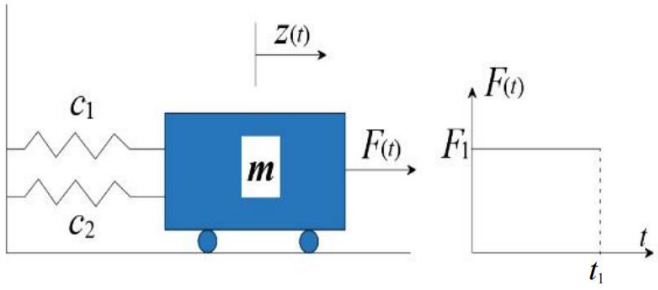

Fig. 6. A nonlinear oscillator.

Table 4. Random variables of Example 3.

Variables	Distribution type	Mean	Standard deviation
m	Normal	1	0.05
C_1	Normal	1	0.1
C_2	Normal	0.1	0.01
r	Normal	0.5	0.05
t_1	Normal	1	0.2
F_1 (Case 1)	Normal	1	0.2
F_1 (Case 2)	Normal	0.6	0.1
F_1 (Case 3)	Normal	0.45	0.075

The reference result is obtained using MCS with a sample size of 1×10^6 and the corresponding probability of failure is 2.859×10^{-2}. The results of the proposed method are compared with those calculated by AK-MCS+U, AK-MCS+EFF, ESC+U, ESC+EFF, AKSE, and AKSE-b [45]. In addition, the results of

RSM combining SS or IS, the active learning reliability methods AK-MSS [46], and AWL-MCS [47] are also listed in Table 5.

Table 5 shows that the listed active learning methods all acquire high-precision failure probabilities, among which the AK-SS requires the largest number of functional calls for this case and the proposed method needs the fewest number of functional calls. The computational efficiency of the proposed method increases by 10 times compared with the AK-SS. Although the efficiency and accuracy of the RSM are improved to a certain extent by combining the response surface with DS and IS, the relative error of the failure probability is still more than 10%. For this case, the proposed method exhibits excellent performance both in terms of accuracy and efficiency, which fully demonstrates the effectiveness of the proposed learning function and selected convergence criteria.

Table 5. Comparison of reliability analysis results for Case 1 in Example 3.

Methods	N_{call}	$\hat{P}_f$	β	$\varepsilon_{PF}(\%)$
MCS	10^6	2.859×10^{-2}	1.902	-
AK-MCS+U	147.2	2.850×10^{-2}	1.903	0.31
AK-MCS+EFF	126.8	2.867×10^{-2}	1.901	0.28
AK-SS	410	2.833×10^{-2}	1.906	0.91
AK-MSS	86	2.870×10^{-2}	1.900	0.38
AWL-MCS	65	2.826×10^{-2}	1.907	1.15
ESC+U	56.2	2.866×10^{-2}	1.901	0.24
ESC+EFF	81.8	2.861×10^{-2}	1.902	0.07
AKSE	38.6	2.862×10^{-2}	1.902	0.10
AKSE-b	42	2.851×10^{-2}	1.903	0.28
Response Surface-DS	62	3.400×10^{-2}	1.820	18.92
Response Surface-IS	109	2.500×10^{-2}	1.960	12.56
Proposed method	35	2.871×10^{-2}	1.900	0.42

In the proposed method, the proposed learning function REI is used to provide a new point for updating the surrogate model. To investigate the compatibility of the proposed method with REI, the reliability analysis results of case 1 in Example 3 by the proposed new response surface model with different learning functions are depicted in Fig. 7, where the scale on the horizontal coordinate is the abbreviation of the different learning functions.

The results in Fig. 7 show the proposed method is sensitive to different learning functions in terms of the functional calls and the failure probability results. The number of functional calls in the ERF and the probability of failure in the EFF both generated outliers. It can be observed in Fig. 7 (a) that the median line of the REI is closer to the red dotted line. Although learning functions U and EI can provide relatively accurate failure probability results, the volatility of the results is significant. From Fig. 7 (b), the learning function EI has the highest fluctuation in the number of functional calls, and the REI is more stable, mainly concentrated between 32 and 37. Overall, the proposed learning function REI provides more stable results in terms of both efficiency and accuracy.

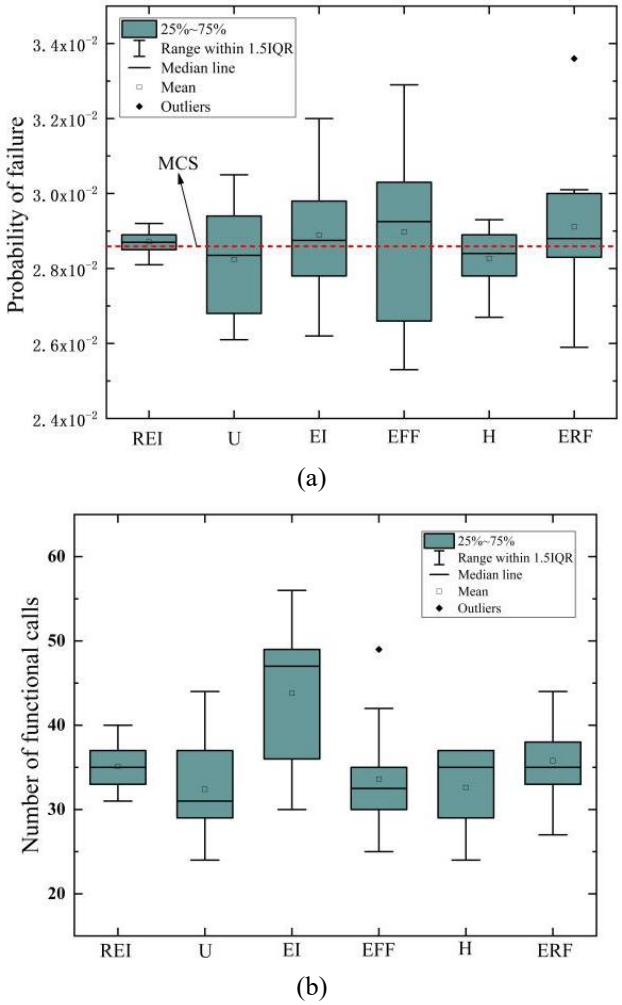

Fig. 7. Boxplots for different methods: (a) Boxplot for the probability of failure with different methods, (b) Boxplot for N_{call} with different methods.

This part focuses on two cases of rare failure in Example 3 to examine the viability of the proposed method. The reference results by MCS are from Reference [48], where the sample sizes are 1.8×10^8 and 9×10^{10}, respectively, and the corresponding failure probability are 9.090×10^{-6} and 1.550×10^{-8}, respectively. The performance of the proposed method for two cases is illustrated in Tables 6 and 7, and the results by AK-

ARBIS [48], AK-MCS, and AKSE [45] are compared.

It is difficult for AK-MCS to achieve the estimation of failure probability less than 10^{-6} because the calculating process is time-consuming to select the best points from the rapidly increasing samples [48]. Although the combination of AK-MCS and IS improves the time-consuming problem to some extent, it still requires multiple functional calls to obtain an exact solution. In cases 2 and 3, AK-IS+EFF needs to call the function 126.8 and 164.7 times, respectively, to obtain the convergent failure probability results. The new stopping criterion ESC and AKSE in the adaptive Kriging method has greatly improved the efficiency of AK-IS, but the relative error is also increased accordingly. For the failure probability of case 3, the relative error of the failure probability by ESC and AKSE-b methods are both more than 5%. It is noted that the number of functional calls of the proposed method is insensitive to the variety of the small failure probability. For all the cases in Example 3, the change in the number of function calls for each case compared to the previous case is less than 5.8%, of which the maximum relative error is less than 3.3%. Overall, the applicability and effectiveness of the proposed method for rare failure events have been demonstrated through Example 3.

Table 6. Reliability analysis results of Case 2 in Example 3.

Methods	N_{call}	$\hat{P}_f$	β	$\varepsilon_{PF}(\%)$
MCS	1.8×10^{8}	9.090×10^{-6}	4.286	-
AK-IS+U	281.6	9.108×10^{-6}	4.286	0.20
AK-IS+EFF	126.8	9.161×10^{-6}	4.284	0.78
AK-ARBIS	71	9.090×10^{-6}	4.286	0
ESC-IS+U	56.2	9.178×10^{-6}	4.284	0.97
ESC-IS+EFF	81.8	9.240×10^{-6}	4.283	1.65
AKSE-IS	47.2	9.032×10^{-6}	4.288	0.64
AKSE-b-IS	49.3	9.130×10^{-6}	4.285	0.44
Proposed method-IS	37	8.998×10^{-6}	4.288	1.01

Table 7. Reliability analysis results of Case 3 in Example 3.

Methods	N_{call}	$\hat{P}_f$	β	$\varepsilon_{PF}(\%)$
MCS	9×10^{10}	1.550×10^{-8}	5.536	-
AK-IS+U	244	1.547×10^{-8}	5.536	0.19
AK-IS+EFF	164.7	1.535×10^{-8}	5.538	0.97
AK-ARBIS	76	1.560×10^{-8}	5.535	0.65
ESC-IS+U	54.7	1.533×10^{-8}	5.538	1.10
ESC-IS+EFF	80.7	1.666×10^{-8}	5.524	7.48
AKSE-IS	48.4	1.518×10^{-8}	5.539	2.06
AKSE-b-IS	61.5	1.447×10^{-8}	5.548	6.65
Proposed method-IS	38.5	1.499×10^{-8}	5.542	3.29

4.4. Example 4: A planar ten-bar structure

This example considers a cantilever tube structure with 9 random variables. As shown in Fig. 8, the structure is subjected to the influence of three concentrated forces F_1, F_2, P, and a torque T. To ensure the reliability of the cantilever tube, it is necessary to ensure that the maximum stress acting on the cantilever tube is less than the allowable threshold. Therefore, the functional function of the structure is defined as

$$G(\mathbf{x}) = S_y - \sigma_{max} \tag{34}$$

where S_y is the yield strength, σ_{max} is the maximum stress on the cantilever tube, which can be calculated according to the fourth strength theory:

$$\sigma_{max} = \sqrt{\sigma_x^2 + 3\tau_{zx}^2} \tag{35}$$

where σ_x and τ_{zx} represent the normal stress and torsional stress on the top surface of the cantilever tube at the origin position, respectively. σ_x and τ_{zx} are specifically calculated as

$$\sigma_x = \frac{P+F_1 \sin\theta_1+F_2 \sin\theta_2}{A} + \frac{Md}{2I} \tag{36}$$

$$\tau_{zx} = \frac{Td}{4I} \tag{37}$$

where A is the surface area of the pipe mouth, M is the cantilever tube subject to bending moment, and I is the extreme moment of inertia. Their calculation formulas are

$$M = F_1 L_1 \cos\theta_1 + F_2 L_2 \cos\theta_2 \tag{38}$$

$$A = \frac{\pi}{4}[d^2 - (d-2t)^2] \tag{39}$$

$$I = \frac{\pi}{64}[d^4 - (d-2t)^4] \tag{40}$$

where L_1 and L_2 are the force arms of the concentrated forces F_1 and F_2, respectively. Table 8 shows the uncertainty states of random variables in the cantilever tube.

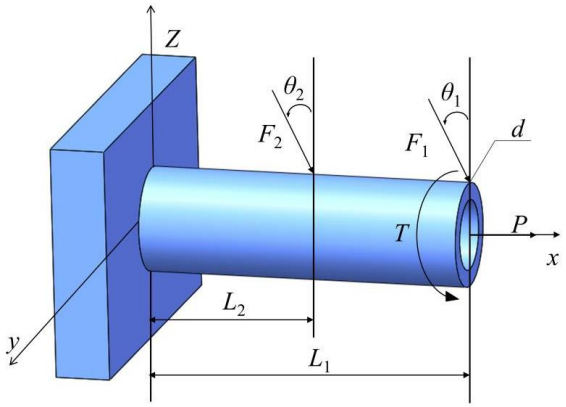

Fig. 8. The cantilever tube and involved variables.

Table 8. Random variables and corresponding parameters of the

cantilever tubal structure

Variables	Distribution type	Parameter 1	Parameter 2
t (mm)	Normal	5.0	0.1
d (mm)	Normal	42.0	0.5
F_1 (kN)	Normal	3.0	0.3
F_2 (kN)	Normal	3.0	0.3
T (Nm)	Normal	90.0	9
S_y(MPa)	Normal	220	22.0
P (kN)	Gumbel	27.0	2.7
L_1 (mm)	Uniform	119.75	120.25
L_2 (mm)	Uniform	59.75	60.25

Note: For normal distribution, Parameters 1 and 2 represent mean and standard deviation, for Gumbel distribution, Parameters 1 and 2 represent location and scale parameters, for uniform distribution, Parameters 1 and 2 represent lower and upper bounds, respectively.

Table 9. Computational results by different methods for Example 4.

Methods	N_{call}	$\hat{P}_f$	β	ε_{PF}(%)
MCS	10^7	6.8226×10^{-3}	2.4665	-
AK-EFF	106.10	6.8278×10^{-3}	2.4662	0.08
AK-U	108.5	6.8180×10^{-3}	2.4667	0.07
AK-FNEIF	79.30	6.8309×10^{-3}	2.4660	0.12
Proposed method	65.5	6.8580×10^{-3}	2.4646	0.52

The reference results by MCS, AK-EFF, AK-U, and AK-FNEIF are from Reference [49], where the sample size is 1×10^7. This example involves a high-dimensional problem with multiple distribution types. It can be seen form Table 9 that the classic AK-MCS method has achieved a higher precision in the assessment of failure probabilities by combining different learning functions and has also improved efficiency. The proposed method has similarly obtained satisfactory results when dealing with this problem, with significant efficiency improvements. By averaging over 65.5 calls to LSF, the proposed method obtained failure assessment results with an error of less than 1%.

4.5. Example 5: A planar ten-bar structure

This example is a planar ten-bar structure with implicit input-output relationships, and its structural schematic is shown in Fig. 9. The lengths of all members are L, the section area of each bar is $A_i(i = 1,2,\cdots,10)$, the elastic modulus is E, and the external load is $P_i(i = 1,2,3)$. Assuming L, E, $A_i(i = 1,2,\cdots,10)$, and $P_i(i = 1,2,3)$ are all random normally distributed, the distribution parameters are shown in Table 10. Establish a limit state function with a vertical displacement D of node 3 not exceeding 3.5 mm: $g(x) = 0.0035 - G(x)$. The reference result for this case is obtained using MCS with a sample size of 3×10^5 and the corresponding probability of failure is 0.0678 [44]. The results of the proposed method compared with other methods are also listed in Table 11.

Table 10. Distribution parameters of the input variables of the ten-bar structure.

Random variables	Mean	Coefficient of variation
L (m)	1	0.05
E (GPa)	100	0.05
A_i (m^2)	0.001	0.15
P_1 (KN)	80	0.05
P_2 (KN)	10	0.05
P_3 (KN)	10	0.05

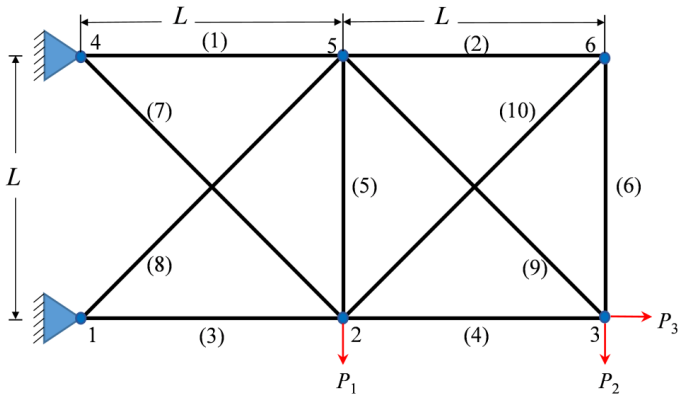

Fig. 9. A truss with ten members.

Table 11. Results of the reliability analysis for Example 5.

Methods	N_{call}	$\hat{P}_f$	ε_{PF}(%)
MCS	3×10^5	0.0678	/
SS	10^5	0.0671	1.01
Ori-Kriging	329	0.0683	0.74
RVM-C	98	0.0680	0.74
Adv-Kriging	83	0.0672	0.88
Proposed method	55	0.0670	1.12

According to the results in Table 11, although SS achieved relatively accurate results, it brings too much computation [50]. In contrast, the listed other methods can reach a good trade-off between accuracy and efficiency. Among them, the Ori-Kriging method has called 329 times finite element calculations and obtained close results [44]. Adv-Kriging is an active learning method based on an advanced Kriging model, which requires 83 calls of finite element analysis to obtain approximate results [44]. Compared to Ori-Kriging, Adv-Kriging has greatly improved the efficiency of solving problems. In addition, RVM-C utilizes correlation vector machines to approximate actual limit state functions and has greatly improved efficiency

compared to SS and Ori-Kriging [51]. It is noted that the proposed method yields an estimation with high accuracy using the least number of calls for finite elements. Overall, from the mentioned examples, the proposed method can provide efficient calculations with accurate results for structural reliability problems.

5. Conclusions

This paper proposes an active learning method for structural reliability analysis combining the response surface model with the Gaussian process of residual fitting and reliability-based sequential sampling design. This strategy predicts residuals generated by RSM using GP models and incorporates the predicted residuals into the constructed response surface model, thus greatly improving the prediction accuracy of RSM. The proposed RMUDM is used to construct the initial response surface model, which improves the construction efficiency and accuracy. The proposed REI function provides a more stable guarantee in terms of efficiency and accuracy for updating the response surface model and GP model. The proposed method can be integrated with IS for rare failure probability events.

Compared with traditional RSMs, the proposed method has greatly improved the accuracy of failure probability assessment, especially for strongly nonlinear problems. Compared with some existing active learning methods, the proposed method shows outstanding efficiency and faster convergence for both strongly nonlinear and rare failure probability problems. In addition, the proposed method can be combined with other sampling methods and learning functions, which fully demonstrates its applicability and effectiveness.

In this paper, the GP model is used to predict the response surface residuals, and it also has the limitations of the GP surrogate model. In actual engineering applications, the uncertainty of the parameter distribution patterns will affect the applicability of the proposed method. However, the basic idea of using surrogate models for residual adaptive fitting is general and applicable to different types of surrogate models. Future research will explore more efficient and accurate adaptive residual prediction methods under different application conditions, and continue to develop more complex actual engineering application models.

Acknowledgments

This work is supported by National Natural Science Foundation of China (No. 52371361, 51879026), Dalian Science and Technology Innovation Fund Project (No. 2020JJ25CY016), and the Fundamental Research Funds for the Central Universities of China (No. 3132023516). And this research is also supported by Key Laboratory for Polar Safety Assurance Technology and Equipment of Liaoning Province.

References

1. Zhou S, Zhang JG, You LF, Zhang QY. Uncertainty propagation in structural reliability with implicit limit state functions under aleatory and epistemic uncertainties. Eksploatacja i Niezawodność – Maintenance and Reliability 2021; 23(2): 231-241. https://doi.org/10.17531/ein.2021.2.3.
2. Peng CL, Chen C, Guo T, Xu WJ. AK-SEUR: An adaptive Kriging-based learning function for structural reliability analysis through sample-based expected uncertainty reduction. Structural Safety 2024; 106: 102384. https://doi.org/10.1016/j.strusafe.2023.102384.
3. Zhao YG, Ono T. A general procedure for first/second-order reliability method (FORM/SORM). Structural Safety 1999; 21: 95-112. https://doi.org/10.1016/s0167-4730(99)00008-9.
4. Lu ZH, Hu DZ, Zhao YG. Second-order Fourth-Moment Method for Structural Reliability. Journal of Engineering Mechanics 2017; 143: 06016010. https://doi.org/10.1061/(asce)em.1943-7889.0001199.
5. Meng Z, Wan HP, Sheng ZL, Li G. A novel study of structural reliability analysis and optimization for super parametric convex model. International Journal for Numerical Methods in Engineering 2020; 121: 4208-4229. http:/dx.doi.org/10.1002/nme.6437.
6. Luo CQ, Keshtegar B, Zhu SP, Taylan Osmanet, Liu XP. Hybrid enhanced Monte Carlo simulation coupled with advanced machine learning approach for accurate and efficient structural reliability analysis. Computer Methods in Applied Mechanics and Engineering 2022; 388: 114218. https://doi.org/10.1016/J.CMA.2021.114218
7. Zhang JH, Xiao M, Gao L, Chu S. Combined projection-outline-based active learning Kriging and adaptive importance sampling method

for hybrid reliability analysis with small failure probabilities. Computer Methods in Applied Mechanics and Engineering 2019; 344: 13-33. http://dx.doi.org/10.1016/j.cma.2018.10.003.

8. Xie JY, Tian ZR, Zhi PP, Zhao YD. Reliability analysis method of coupling optimal importance sampling density and multi-fidelity Kriging model. Eksploatacja i Niezawodność – Maintenance and Reliability 2023; 25(2): 161893. https://doi.org/10.17531/ein/161893.
9. Nguyen T-T, Dang V-H, Nguyen H-X. Efficient framework for structural reliability analysis based on adaptive ensemble learning paired with subset simulation. Structures 2022; 45: 1738-1750. https://doi.org/10.1016/j.istruc.2022.09.072.
10. Morio J, Balesdent M, Jacquemart D, Vergé C. A survey of rare event simulation methods for static input-output models. Simulation Modelling Practice and Theory 2014; 49: 287-304. https://doi.org/10.1016/j.simpat.2014.10.007.
11. Grooteman F. An adaptive directional importance sampling method for structural reliability. Probabilistic Engineering Mechanics 2011; 26: 134-141. http://dx.doi.org/10.1016/j.probengmech.2010.11.002.
12. Keshtegar B. Chaotic conjugate stability transformation method for structural reliability analysis. Computer Methods in Applied Mechanics and Engineering 2016; 310: 866-885. http://dx.doi.org/10.1016/j.cma.2016.07.046.
13. Gao SZ, Zhao YK, Zhao XD, Zhang YM. Application of response surface method based on new strategy in structural reliability analysis. Structures 2023; 57: 105202. https://doi.org/10.1016/j.istruc.2023.105202.
14. Alibrandi U. A response surface method for stochastic dynamic analysis. Reliability Engineering and System Safety 2014; 126: 44-53. https://doi.org/10.1016/j.ress.2014.01.003.
15. Sajad AS, Fatemeh E, Xu XY, Liang XH. Machine learning-based methods in structural reliability analysis: A review. Reliability Engineering and System Safety 2022; 219: 108223. https://doi.org/10.1016/j.ress.2021.108223.
16. Zhang YM, Ma J, Du WY. A new radial basis function active learning method based on distance constraint for structural reliability analysis. International Journal of Mechanics and Materials in Design 2023; 19(3): 567-581. https://doi.org/10.1007/S10999-023-09644-X.
17. Liu H, Xiao CN. Global non-probabilistic reliability sensitivity analysis based on surrogate model. Eksploatacja i Niezawodność – Maintenance and Reliability 2022; 24(4): 612-616. https://doi.org/10.17531/ein.2022.4.2.
18. Chen PY, Zhao CB, Yao H, Zhao SN. An adaptive method based on PC-Kriging for system reliability analysis of truss structures. Eksploatacja i Niezawodność – Maintenance and Reliability 2023; 25(3): 169497. https://doi.org/10.17531/ein/169497.
19. Alibrandi U, Alani AM, Ricciardi G. A new sampling strategy for SVM-based response surface for structural reliability analysis. Probabilistic Engineering Mechanics 2015; 41: 1-12. https://doi.org/10.1016/j.probengmech.2015.04.001.
20. Atin R, Subrata C. Support vector machine in structural reliability analysis: A review. Reliability Engineering and System Safety 2023; 233: 109126. https://doi.org/10.1016/j.ress.2023.109126.
21. Li K, Tang KJ, Li JL, et al. A hierarchical neural hybrid method for failure probability estimation. IEEE Access 2019; 7: 112087-112096. https://doi.org/10.1109/ACCESS.2019.2934980
22. Chao R, Younes A, Didier L, et al. Ensemble of surrogates combining Kriging and Artificial Neural Networks for reliability analysis with local goodness measurement. Structural Safety 2022; 96: 102186. https://doi.org/10.1016/j.strusafe.2022.102186.
23. David W, Carmine G. Gaussian process regression for fatigue reliability analysis of offshore wind turbines. Structural Safety 2021; 88: 102020. https://doi.org/10.1016/j.strusafe.2020.102020.
24. Liu D, Wang SP, Zhang C, Tomovic M. Bayesian model averaging based reliability analysis method for monotonic degradation dataset based on inverse Gaussian process and Gamma process. Reliability Engineering and System Safety 2018; 180: 25-38. https://doi.org/10.1016/j.ress.2018.06.019.
25. Xia Y, Wang YM. Improved Hybrid Response Surface Method Based on Double Weighted Regression and Vector Projection. Mathematical Problems in Engineering 2022; 2022: 5104027. https://doi.org/10.1155/2022/5104027.
26. Zhou D, Pan E, Zhang YM. Fractional polynomial function in stochastic response surface method for reliability analysis. Journal of Mechanical Science and Technology 2021; 35(1): 121-131. https://doi.org/10.1007/S12206-020-1211-3.
27. Xia Y, Kong WZ, Yu YY, Hu YY, Li JY. Improved Response Surface Method Based on Linear Gradient Iterative Criterion. Advances in Civil Engineering 2023; 023: 6360796. https://doi.org/10.1155/2023/6360796.
28. Roussouly N, Petitjean F, Salaun M. A new adaptive response surface method for reliability analysis. Probabilistic Engineering Mechanics 2013; 32: 103-115. https://doi.org/10.1016/j.probengmech.2012.10.001.

29. Li P, Hu SX, Li HY, Yang SQ, Wen HX. An improved quasi-sparse response surface model using the weighting method for low-dimensional simulation. Applied Soft Computing Journal 2019; 85: 105883-105883. https://doi.org/10.1016/j.asoc.2019.105883.
30. Romero VJ, Swiler LP, Giunta AA. Construction of response surfaces based on progressive-lattice-sampling experimental designs with application to uncertainty propagation. Structural Safety 2004; 26(2): 201-209. https://doi.org/10.1016/j.strusafe.2003.03.001.
31. Rathi KA, Sharma SVP, Chakraborty A. Sequential Stochastic Response Surface Method Using Moving Least Squares-Based Sparse Grid Scheme for Efficient Reliability Analysis. International Journal of Computational Methods 2019; 16(5): 38. https://doi.org/10.1142/S0219876218400170.
32. Myridis NE. Stochastic processes: theory for applications, by Robert G. Gallager. Contemporary Physics 2016; 57(2): 264-265. https://doi.org/10.1080/00107514.2015.1133711.
33. Chen C, Liao Q. ANOVA Gaussian process modeling for high-dimensional stochastic computational models. Journal of Computational Physics 2020; 416: 109519. https://doi.org/0.1016/j.jcp.2020.109519.
34. Gao HF, Fei CW, Bai GC, Ding BL. Reliability-based low-cycle fatigue damage analysis for turbine blade with thermo-structural interaction. Aerospace Science and Technology 2016; 49: 289-300. https://doi.org/10.1016/j.ast.2015.12.017.
35. Song ZZ, Liu Z, Zhang HY, Zhu P. An improved sufficient dimension reduction-based Kriging modeling method for high-dimensional evaluation-expensive problems. Computer Methods in Applied Mechanics and Engineering 2024; 418: 116544. https://doi.org/10.1016/j.cma.2023.116544.
36. Li YT, Luo YJ, Zhong Z. An active sparse polynomial chaos expansion approach based on sequential relevance vector machine, Computer Methods in Applied Mechanics and Engineering 2024; 418: 116554. https://doi.org/10.1016/j.cma.2023.116554.
37. Gao Y, Wang X. An effective warpage optimization method in injection molding based on the Kriging model. The International Journal of Advanced Manufacturing Technology 2008; 37: 953-960. https://doi.org/10.1007/s00170-007-1044-6.
38. Ranjan P, Haynes R, Karsten R. A Computationally Stable Approach to Gaussian Process Interpolation of Deterministic Computer Simulation Data. Technometrics 2011; 53(4): 366-378. https://doi.org/10.1198/TECH.2011.09141.
39. Jones RD, Schonlau M, Welch JW. Efficient Global Optimization of Expensive Black-Box Functions. Journal of Global Optimization 1998; 13(4): 455-492. https://doi.org/10.1023/A:1008306431147
40. Zhi PP, Wang ZL, Li YH, Tian ZR. RMQGS-APS-Kriging-based Active Learning Structural Reliability Analysis Method. Journal of Mechanical Engineering (Chinese) 2022; 58(16): 420-429. https://doi.org/10.3901/JME.2022.16.420
41. Meng Z, Zhang ZH, Li G, Zhang DQ. An active weight learning method for efficient reliability assessment with small failure probability. Structural and Multidisciplinary Optimization 2020; 61(3): 1157-1170. https://doi.org/10.1007/s00158-019-02419-z.
42. Xiao NC, Zuo MJ, Guo W. Efficient reliability analysis based on adaptive sequential sampling design and cross-validation. Applied Mathematical Modelling 2018; 58: 404-420. https://doi.org/10.1016/j.apm.2018.02.012.
43. Zheng PJ, Wang CM, Zong ZH, Wang LQ. A new active learning method based on the learning function U of the AK-MCS reliability analysis method. Engineering Structures 2017; 148: 185-194. https://doi.org/10.1016/j.engstruct.2017.06.038.
44. Zhang LG, Lu ZZ, Wang P. Efficient structural reliability analysis method based on advanced Kriging model. Applied Mathematical Modelling 2015; 39(2): 781-793. https://doi.org/10.1016/j.apm.2014.07.008.
45. Wang JS, Xu GJ, Li YL, Ahsan K. AKSE: A novel adaptive Kriging method combining sampling region scheme and error-based stopping criterion for structural reliability analysis. Reliability Engineering and System Safety 2022; 219: 108214. https://doi.org/10.1016/J.RESS.2021.108214.
46. Xu CL, Chen WD, Ma JX, Shi YQ, Lu SZ. AK-MSS: An adaptation of the AK-MCS method for small failure probabilities. Structural Safety 2020; 86: 101971. https://doi.org/10.1016/j.strusafe.2020.101971.
47. Meng Z, Zhang ZH, Li G, Zhang DQ. An active weight learning method for efficient reliability assessment with small failure probability. Structural and Multidisciplinary Optimization 2020; 61(3): 1157-1170. https://doi.org/10.1007/s00158-019-02419-z.
48. Yun WY, Lu ZZ, Jiang X, Zhang LG, He PF. AK-ARBIS: An improved AK-MCS based on the adaptive radial-based importance sampling for small failure probability. Structural Safety 2020; 82: 101891. https://doi.org/10.1016/j.strusafe.2019.101891.
49. Wen ZX ,Pei HQ ,Liu H , et al. A Sequential Kriging reliability analysis method with characteristics of adaptive sampling regions and parallelizability. Reliability Engineering and System Safety, 2016; 153: 170-179. https://doi.org/10.1016/j.ress.2016.05.002.

50. Au SK, Beck JL. Estimation of small failure probabilities in high dimension by subset simulation. Probabilistic Engineering Mechanics 2001; 16(4): 263-277. https://doi.org/10.1016/S0266-8920(01)00019-4.
51. Zhou CC, Lu ZZ, Yuan LX. Use of Relevance Vector Machine in Structural Reliability Analysis. Journal of aircraft 2013; 50(6): 1726-1733. https://doi.org/10.2514/1.C031950.